NONLINEAR SINGLE-MODE PANEL FLUTTER AT CONTINOUSLY VARYING FLIGHT SPEED

Anastasia Shishaeva[+1], Vasily Vedeneev[+2], and Andrey Aksenov[+3]
[+1,2]Lomonosov Moscow State University, Moscow, Russia
[+1,3]Tesis LTD, Moscow, Russia

Instability of elastic plate in unsteady sub- and supersonic flow is studied. The observe various limit cycle oscillations of the plate for different rates of increase and decrease of the flow speed. A number of the limit cycles bifurcations is detected and analysed.

Keyword: panel flutter, single mode flutter, internal resonance, nonlinear oscillations.

1. INTRODUCTION

Aeroelastic instability of skin panels, known as panel flutter, has been intensively studied over decades [1-6]. At high supersonic speeds the coupled-mode panel flutter occurs, while at low supersonic speeds the single-mode flutter is dominating. The coupled-mode flutter was investigated in details in the 1960th [1-2]. The single-mode flutter was studied during last ten years [7-12]. Recent nonlinear study [13] has shown that at small supersonic flight speeds, different limit cycles can coexist at the same flight conditions, which is caused by linear growth mechanism and nonlinear interaction between growing eigenmodes. Some of the limit cycles include internal resonance between natural modes. Switches of panel oscillations from one limit cycles to another is accompanied by bifurcation of the aeroelastic dynamic system. In the present paper we study such bifurcations by continuously changing the flow speed at various rates, and watching the panel response. This approach gives an explicit way to note the bifurcations in the limit cycles and reveals additional bifurcations not noticed before.

2. PROBLEM FORMULATION

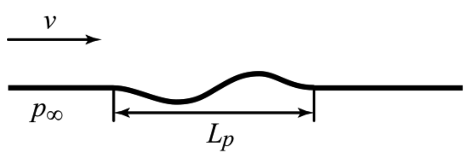

Figure 1. Plate in a gas flow

The formulation of the problem is as follows. The elastic plate of length $L_p = 0.3$ m and thickness $h_p = 0.001$ m is mounted into a rigid plane (Figure 1). The plate is made of steel with Young's modulus $E = 2 \times 10^{11}$ Pa, Poison coefficient $\nu = 0.3$ and density $\rho_m = 7800$ kg/m^3. In dimensionless terms, the plate stiffness and length are:

$$D = D_p/(a^2 \rho_m h^3) = 21.4, \; L = L_p/h_p = 300,$$

Where $D_p = Eh^3/(12(1-\nu))$ is the dimensional plate stiffness, and $a = 331$ m/s is the speed of sound in the air. Similar values of dimensionless parameters correspond to other metal materials (e.g., aluminium and titanium). The plate is governed by the nonlinear Mindlin plate model, where elastic strains are calculated through Koiter–Sanders shell theory.

[+1]anastasiashishaeva@rambler.ru, [+2]vasily@vedeneev.ru, [+3]andrey@tesis.com.ru

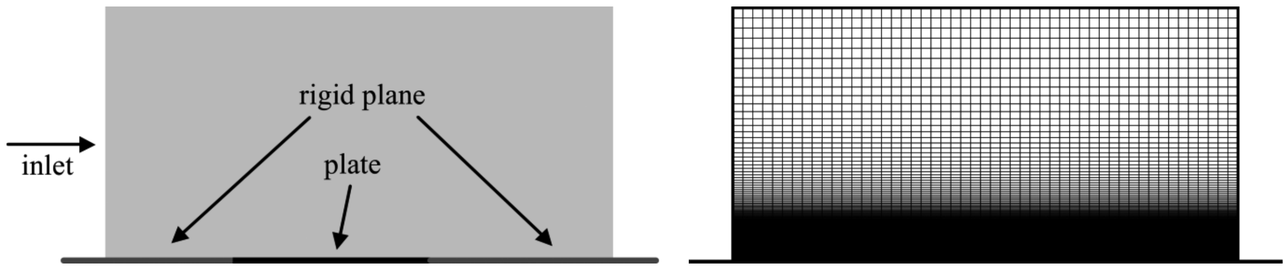

Figure 2. Simulation domain (a) and computational grid (b) in FlowVision

The simulation domain of the gas flow is a rectangular 0.6 x 0.3 m (Figure 2a). We consider inviscid perfect gas with air properties assigned. Gas flows over one side of the plate with varying Mach number M(t). At the other side of the plate, a pressure equal to the undisturbed flow pressure is specified, such that the undisturbed pressure difference along the plate is zero. Linear increase and decrease of M between 0.7 and 1.7 during 2.5 s, 5 s, 7.5 s and 10 s is considered. In all simulation, a slight sinusoidal disturbing force is applied to the plate in order to excite each bifurcation of limit cycle oscillation.

Subsequent plate-flow interaction is calculated using two coupled codes, Abaqus for simulating the plate, and FlowVision for simulating the gas flow. Abaqus is a finite-element commercial code originally developed for stress analysis. FlowVision is a finite-volume commercial code developed by Tesis LTD for aero/hydrodynamic applications. Interaction between the codes is organized through direct coupling mechanism along the surface of the deformed plate [14-15]. Both codes are executed in turns; exchanges occur at each time step according to conventional. The displacements and velocities of the plate points are sent from Abaqus to FlowVision, whereas the pressure distribution along the plate surface is sent back from FlowVision to Abaqus. Mesh properties used in the simulation are as follows. The Abaqus plate model consists of hexahedral finite elements, with 60 elements along the chordwise direction. The FlowVision flow model consists of 50x494 (length x height) finite volumes. The vertical size of finite volumes varies from 0.0001 m near the plate to 0.01 m in the far field of the simulation domain (see Figure 2a).

It is convenient to analyze plate behavior by watching deflection y of a reference point plotted versus time. The reference point is located at 0.22 m downstream of the leading edge of the elastic plate, which is approximately 3/4 of the plate length. Fourier analysis is used to calculate the spectra of limit cycles observed.

Investigation of grid, time and domain convergence, testing of the model on coupled and single mode flutter at constant flow speed are described in [13].

3. RESULTS

Our previous investigation of is described in [13]. We investigated plate instability at constant flow speed. We obtained eight bifurcations. They are shown in Table 1 for comparison.

Two series of calculation have been considered in our present investigation. The first corresponds to increase of M, the second corresponds to decrease of M. Results are shown in Table 1, Figure 3 and Figure 4. Nine bifurcations were detected. Here bifurcation sequence corresponds to acceleration. I - pitchfork bifurcation is a static plate divergence. II – Hopf bifurcation is a limit cycle occurrence. We detected first mode limit cycle with freezing. Freezing is a short stop of oscillation during the limit cycle. III – first mode limit cycle without freezing. IV - transition from non-resonant to resonant limit cycle. V – minor bifurcation of resonant limit cycles, VI – transition from resonant limit cycle to high-frequency non-periodic oscillations, VII – transition from high-frequency non-periodic oscillations to third-mode limit cycle, VIII –transition from third-mode limit cycle to first-mode limit cycle, IX - transition to stability. The number and positions of bifurcations vary with intensity and direction of M changing (Table 1). We can see that bifurcations II and III are the same for all accelerations and for constant speed. Bifurcation IV depends on acceleration direction but not on acceleration intensity. Bifurcations VI, VII, VIII, IX are the most sensitive for direction and intensity of acceleration.

Table 1. The list of bifurcation.

	Increase of M						Decrease of M				M = const [13]
	0,5 s	1 s	2,5 s	5 s	7,5 s	10 s	2,5 s	5 s	7,5 s	10 s	
I	0,79	0,79	0,79	0,79	0,8	0,8	0,83	0,83	0,83	0,821	0,7
II	1	1	1	1	1	1	0,97	0,97	0,993	0,993	1
III	-	1,07	1,07	1,07	1,06	1,06	1,07	1,07	1,07	1,07	1,05
IV	1,1	1,1	1,1	1,1	1,1	1,1	1,09	1,09	1,09	1,09	1,12
V	1,24	1,24	1,24	1,23	1,23	1,22	1,17	1,2	1,25	1,165	-
VI	-	-	-	1,45	1,41	1,4	1,19	1,22	1,28	1,27	1,33
VII	-	-	-	-	1,53	1,53	1,2	1,31	1,36	1,36	1,42
VIII	-	1,68	1,6	1,58	1,63	1,63	1,23	1,34	1,37	1,38	1,44
IX	-	-	-	-	1,68	1,68	1,5	1,5	1,46	1,46	1,67

For faster increase of M, some of the limit cycles are not formed, since the formation period is too large. For example, for ΔM=1 during 0.5 s, 1 s and 2.5 s we have only divergence, first mode limit cycles, resonant limit cycle, though more dangerous high-frequency or non-periodic oscillations are missed (see Figure 3a-Figure 3c). For ΔM=1 during 5 s we have the same behavior as in the previous case almost in whole interval, except a small area 1.45<M<1.58, where a high-frequency non-periodic oscillations are formed (see Figure 3d). For ΔM=1 during 7.5 s we have a similar behavior in a low Much number as in previous cases. But for M>1.4 we have a completely difference results. There is a long segment of non-periodic oscillations (1.41<M<1.53) and third-mode limit cycle (1.53<M<1.63) (see Figure 3e). Then, for smaller increase of M (ΔM=1 during 10 s) we have a very similar behavior as in the previous case in the whole interval. Only positions of some bifurcation are slightly different (see Figure 3f).

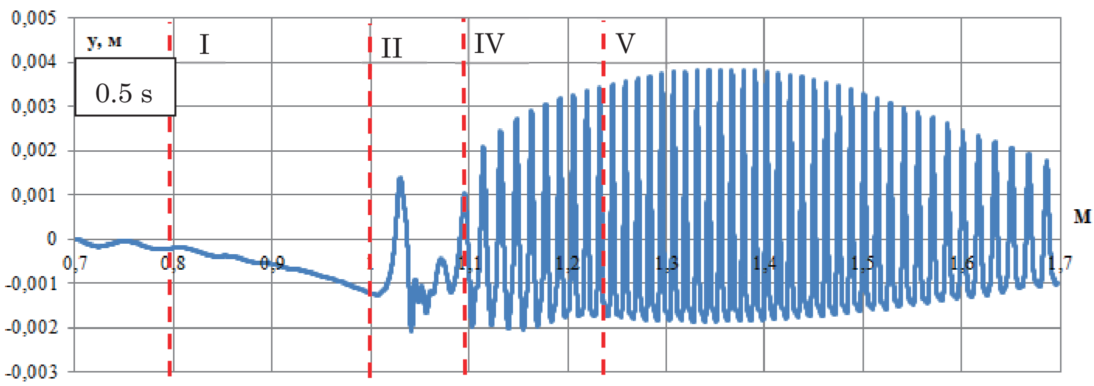

a

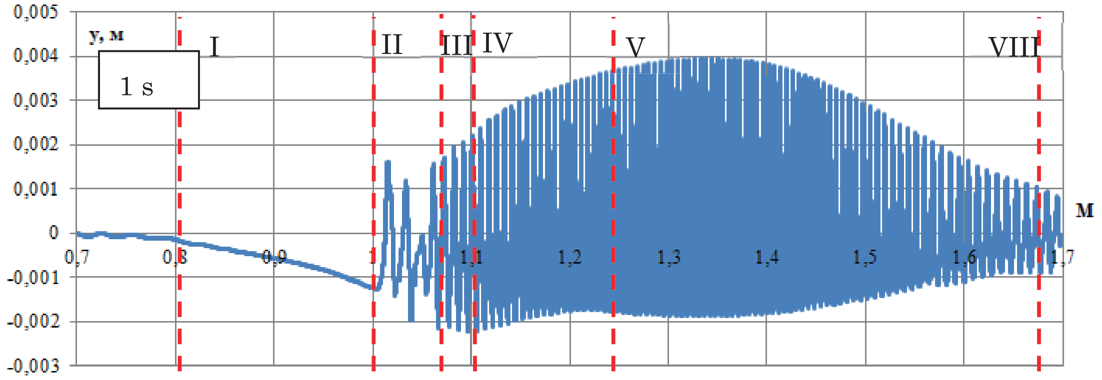
y, м
1 s
I
II
III
IV
V
VIII
м
0,005
0,004
0,003
0,002
0,001
0
-0,001
-0,002
-0,003
0,7
0,8
0,9
1
1,1
1,2
1,3
1,4
1,5
1,6
1,7

b

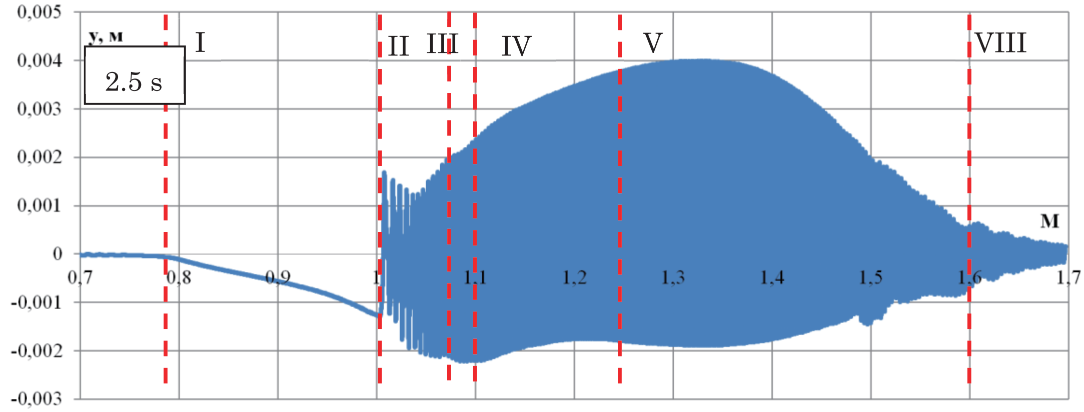
y, м
2.5 s
I
II
III
IV
V
VIII
м
0,005
0,004
0,003
0,002
0,001
0
-0,001
-0,002
-0,003
0,7
0,8
0,9
1
1,1
1,2
1,3
1,4
1,5
1,6
1,7

c

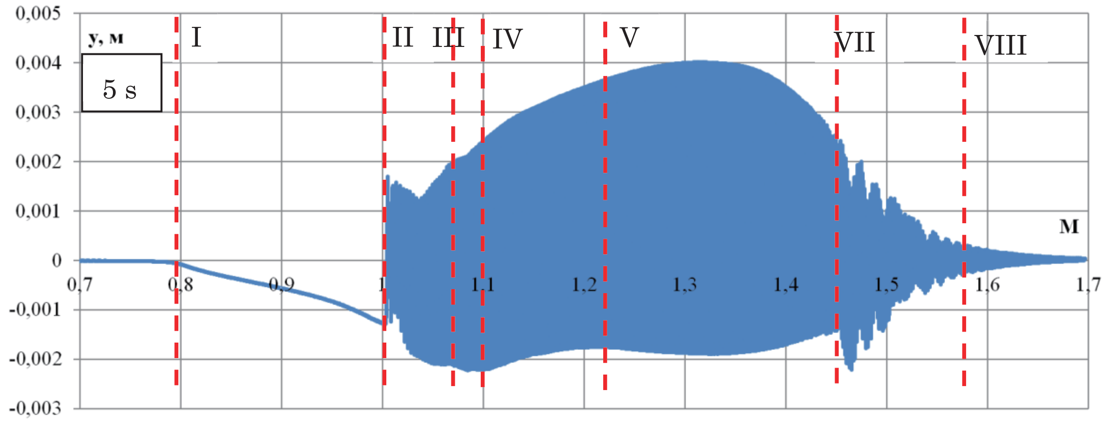
y, м
5 s
I
II
III
IV
V
VII
VIII
м
0,005
0,004
0,003
0,002
0,001
0
-0,001
-0,002
-0,003
0,7
0,8
0,9
1
1,1
1,2
1,3
1,4
1,5
1,6
1,7

d

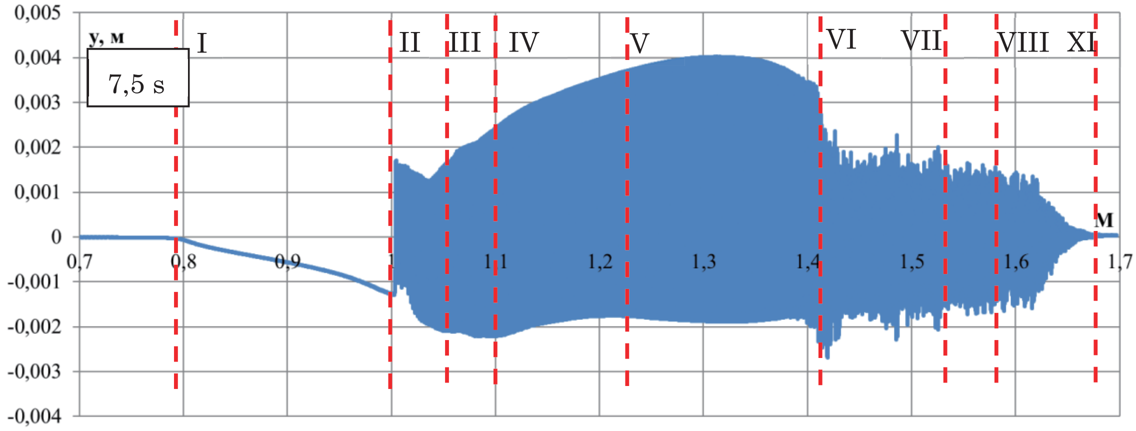

e

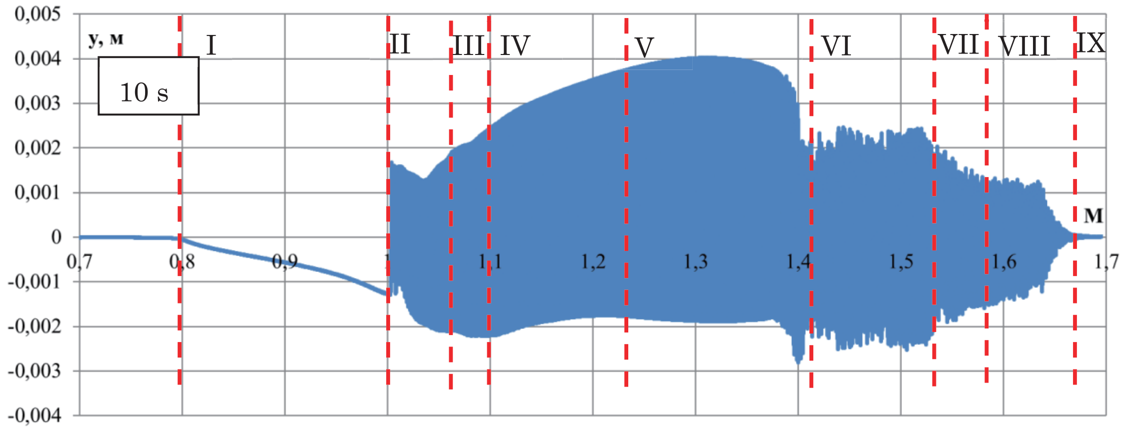

f

Figure 3: Vertical deflection of a plate point vs M in the case of acceleration from M=0.7 to M=1.7 during 0.5 s (a), 1 s (b), 2.5 s (c), 5 s (d), 7.5 s (e), 10 s (f), red lines represent bifurcations of the limit cycle.

Plate instability is significantly different for increase and decrease of M. Thus, in all cases of decrease instability occurs if M<1.5 and may take place till M=0.8, whereas in the case of increase plate become unstable then M>0.8 and can be instable till M=1.7 (see Figure 4). Also there is a significant difference between corresponding rates of increasing and decreasing with the same module of acceleration. For example, for decreasing of M during 2.5 s there is a small area of high-frequency non-periodic oscillations (see Figure 4a) (1.19-1.2), while for increasing of M during 2.5 s there are no high-frequency non-periodic oscillations (see Figure 3a). Further all cases of decrease of M are significantly different from each other for M>1.2 (see Figure 4). Thus, for decreasing of M during 2.5 s there is a big area of first mode limit cycle (1.23<M<1.5) and small areas of non-periodic oscillations and third mode limit cycle (1.19<M<1.2, 1.2<M<1.23) (see Figure 4a), while for decreasing during 5 s there is a big area of non-periodic oscillations (1.22<M<1.31) and shifted area of third mode limit cycle (1.31<M<1.34) (see Figure 4b). For decreasing during 7.5 s the area of non-periodic oscillations is shifted to the high M (1.28<M<1.36), also the region of resonant limit cycle is bigger than in previous cases (1.09<M<1.25) (see Figure 4c). For decreasing during 10 s there is a large region of transition from resonant limit cycle to non-periodic oscillations (1.165<M<1.27) (see Figure 4d).

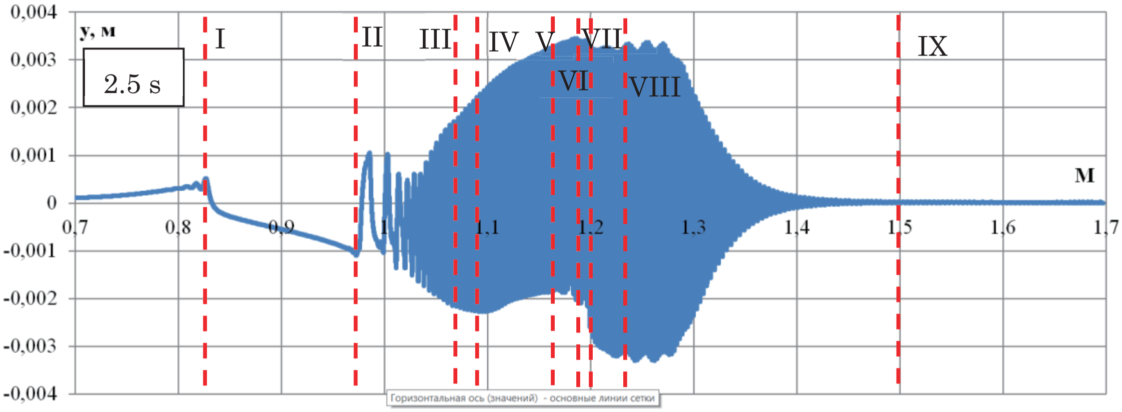
y, м
2.5 s
I
II
III
IV
V
VI
VII
VIII
IX
M
0,004
0,003
0,002
0,001
0
-0,001
-0,002
-0,003
-0,004
0,7
0,8
0,9
1
1,1
1,2
1,3
1,4
1,5
1,6
1,7

a

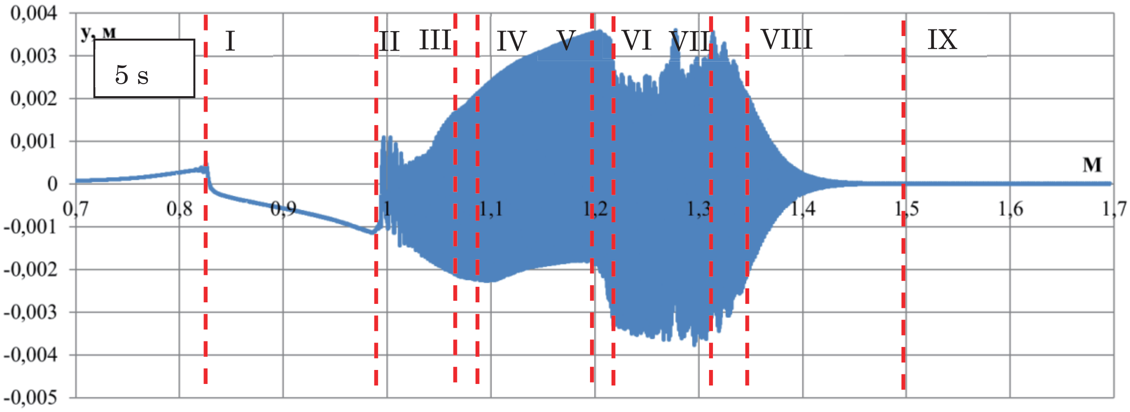
y, м
5 s
I
II
III
IV
V
VI
VII
VIII
IX
M
0,004
0,003
0,002
0,001
0
-0,001
-0,002
-0,003
-0,004
-0,005
0,7
0,8
0,9
1
1,1
1,2
1,3
1,4
1,5
1,6
1,7

b

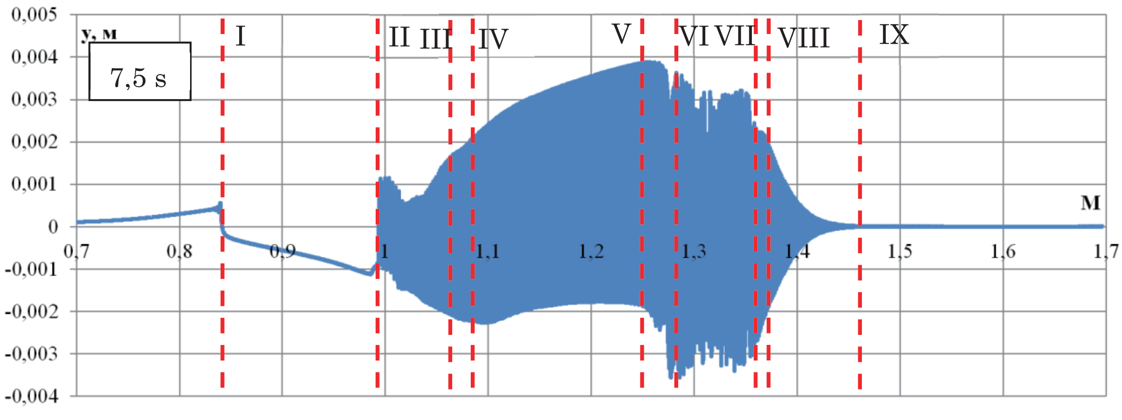
y, м
7,5 s
I
II
III
IV
V
VI
VII
VIII
IX
M
0,005
0,004
0,003
0,002
0,001
0
-0,001
-0,002
-0,003
-0,004
0,7
0,8
0,9
1
1,1
1,2
1,3
1,4
1,5
1,6
1,7

c

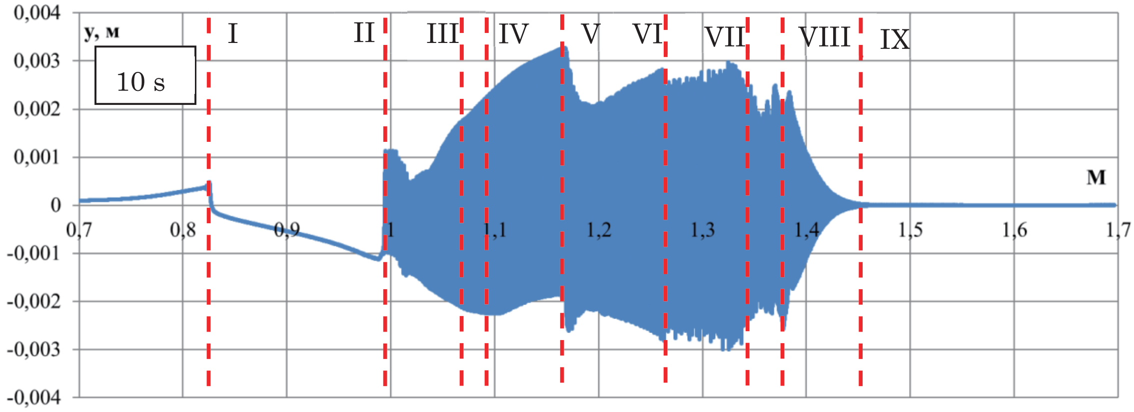

d

Figure 4: Vertical deflection of a plate point vs M in the case of deceleration from M=1.7 to M=0.7 during 2.5 s (a), 5 s (b), 7.5 s (c), 10 s (d), red lines represent bifurcations of the limit cycle.

Summary, we have shown that plate behavior is significantly different in the cases of increase and decrease of a flow speed. We can conclude that hysteresis areas near bifurcation are detected. Beside that, we have obtained that fast increase and decrease of a flow allow avoiding the most dangerous types of flutter, such as high frequency non-periodic flutter or third mode flutter, while slow increase or decrease allows investigating instability area in details. Also, we have obtained that instability occurs at all considered accelerations.

4. CONCLUSIONS

Numerical study of a plate instability in an unsteady flow has been conducted. Ten different rates of the increase and decrease of the flow speed have been investigates. A series of bifurcations for each case is detected. It is shown that fast increase and decrease of a flow speed allows avoiding the most dangerous types of flutter, namely high frequency non-periodic flutter or third mode flutter. However, first mode flutter is not suppressed even for very high accelerations.

ACKNOWLEDGMENT

The work is supported by grant MK-5514.2016.1 and grant MD-4544.2015.1.

REFERENCES

1) Movchan, A.A.,: On stability of a panel moving in a gas. *Prikladnaya Matematika i Mekhanika,* Vol. 21 (2), pp. 231–243, 1957 (in Russian); translated in NASA RE 11-22-58 W, 1959.
2) Bolotin, V.V.: Nonconservative Problems of the Theory of Elastic Stability, Pergamon Press, Oxford, 1963.
3) Dowell, E.H. : Aeroelasticity of Plates and Shells. Noordhoff International Publishing, Leyden. 1974.
4) Dugundji, J. : Theoretical considerations of panel flutter at high supersonic Mach numbers, *AIAA Journal* Vol. 4 (7), pp. 1257–1266, 1966.
5) Grigolyuk, E.I., Lamper, R.E., Shandarov, L.G.: Flutter of plates and shells, *Itogi nauki. Mekhanica. 1963*, VINITI, Moscow, pp. 34–90 (in Russian), 1965.
6) Mei, C., Abdel-Motagaly, K., Chen, R.R.: Review of nonlinear panel flutter at supersonic and hypersonic speeds, *Applied Mechanics Reviews*, Vol. 10, pp. 321–332, 1999.
7) Vedeneev, V.V.: Flutter of a wide strip plate in a supersonic gas flow, *Fluid Dynamics* Vol. 5, 805–817,

2005.
8) Vedeneev, V.V.: Nonlinear high-frequency flutter of a plate, *Fluid Dynamics* Vol. 5, 858–868, 2007.
9) Vedeneev, V.V., Guvernyuk, S.V., Zubkov, A.F., Kolotnikov, M.E., Experimental observation of single mode panel flutter in supersonic gas flow, *Journal of Fluids and Structures,* Vol. 26, 764–779, 2010.
10) Vedeneev, V.V.: Panel flutter at low supersonic speeds, *Journal of Fluids and Structures* Vol. 29, pp. 79–96, 2012.
11) Vedeneev, V.V.: Effect of damping on flutter of simply supported and clamped panels at low supersonic speeds, *Journal of Fluids and Structures* Vol. 40, pp. 366–372, 2013.
12) Vedeneev, V.V.: Limit oscillatory cycles in the single mode flutter of a plate. *Journal of Applied Mathematics and Mechanics*, Vol 77 (3), pp. 257–267, 2013.
13) Shishaeva, A.S., Vedeneev, V.V., Aksenov A.A.: Nonlinear single-mode and multi-mode panel flutter oscillations at low supersonic speeds, *Journal of fluids and structures*, Vol. 56, pp. 205-223, 2015.
14) Aksenov, A.A., Dyadkin, A.A., Pokhilko, V.I.: Overcoming of barrier between CAD and CFD by modified finite volume method. Proceedings of 1998, ASME Pressure Vessels and Piping Division Conference, San Diego, 377-2, pp. 79–86, 1998.
15) Aksenov, A.A, Korenev, D.V, Shishaeva, A.S., Vucinic, D., Mravak, Z.: Drop-Test FSI simulation with Abaqus and FlowVision based on the direct 2-way coupling approach. Proceedings of Abaqus Users' Conference, Newport, Rhode Island, pp. 611–624, 2008.